Electronic Supplementary Material (ESI) for Journal of Materials Chemistry C.


# SUPPORTING INFORMATION

# Luminescent Solar Concentrators with Outstanding Optical Properties by Employment of D-A-D Quinoxaline Fluorophores

Costanza Papucci,[a,b,c] Rima Charaf,[d] Carmen Coppola,[c,e] Adalgisa Sinicropi,[a,c,e] Mariangela di Donato,[a,f] Maria Taddei,[a,f] Paolo Foggi,[f,g,h], Antonella Battisti,[i] Bastiaan de Jong,[c,j] Lorenzo Zani,[a] Alessandro Mordini,[a,b] Andrea Pucci,*[a,d] Massimo Calamante*[a,b] and Gianna Reginato.[a]

*[a] Institute of Chemistry of Organometallic Compounds (CNR-ICCOM), Via Madonna del Piano 10, 50019 Sesto Fiorentino, Italy; [b] Department of Chemistry "U. Schiff", University of Florence, Via della Lastruccia 13, 50019 Sesto Fiorentino, Italy; [c] Department of Biotechnology, Chemistry and Pharmacy, University of Siena, Via A. Moro 2, 53100 Siena, Italy; [d] Department of Chemistry and Industrial Chemistry, University of Pisa, Via G. Moruzzi 13, 56124 Pisa, Italy; [e] CSGI, Consorzio per lo Sviluppo dei Sistemi a Grande Interfase, 50019 Sesto Fiorentino, Italy; [f] LENS, European Laboratory for Non-Linear Spectroscopy, via N. Carrara 1, 50019 Sesto Fiorentino, Italy; [g] Department of Chemistry, Biology and Biotechnology, University of Perugia, via Elce di Sotto 8, 06123 Perugia, Italy; [h] INRIM (Istituto Nazionale di Scienza Metrologica), Strada delle Cacce 91, 10135 Torino, Italy; [i] Istituto Nanoscienze-CNR and NEST-Scuola Normale Superiore, Piazza S. Silvestro 12, 56127 Pisa, Italy; [j] Cicci Research s.r.l. Via Giordania 227, 58100 Grosseto, Italy.*

**Table of Contents**



## 1. Synthesis of compounds 2,5,6,9.

*3,6-Dibromobenzene-1,2-diamine (**2**)*

To a suspension of 4,7-dibromo-2,1,3-benzothiadiazole (**1**) (500 mg, 1.7 mmol, 1.0 eq) in EtOH (85 mL) at 0°C, under atmosphere of $N_2$, $NaBH_4$ (1.16 g, 30.6 mmol, 18.0 eq) was added in four parts. The mixture was stirred at 0°C for 10' and then to room temperature for 16 h. Then, the mixture was cooled at 0°C, and the excess of $NaBH_4$ neutralized with $H_2O$ (15 mL). The mixture was concentrated under reduced pressure to eliminate EtOH and then extracted with $Et_2O$ (2 × 20 mL). The organic phase was washed with brine (30 mL) and dried on anhydrous $Na_2SO_4$. The solvents were removed under reduced pressure and the crude product purified by washing with EtOH, to eliminate the insoluble starting material. The organic solution was filtered and concentrated under vacuum, obtaining the product **2** as white solid (348 mg, 1.32 mmol, 77%). $^1$H-NMR (400 MHz, $CDCl_3$): δ = 6.39 (s, 2H), 4.26 (s, 4H) ppm. Spectroscopic data are in agreement with those reported in the literature.[1]

*5,8-Dibromo-2,3-diphenylquinoxaline (**5**)*

To a solution of diamine **2** (721 mg, 2.7 mmol, 1.0 eq) in EtOH (15 mL), 1,2-di(phenyl)etan-1,2-dione **3** (567 mg, 2.7 mmol, 1.0 eq) was added under inert atmosphere. The mixture was heated to reflux and stirred for 24 h. The obtained precipitate was recovered by filtration, washed and dried under vacuum, obtaining the product **5** as a pale yellow solid (761 mg, 1.74 mmol, 67%). $^{1}$H-NMR (400 MHz, $CDCl_3$) δ = 7.91 (s, 2H); 7.65-7.67; (m, 4H); 7.34-7.43 (m, 6 H) ppm. Spectroscopic data are in agreement with those reported in literature.[2]

*5,8-Dibromo-2,3-dihexylquinoxaline (**6**)*

To a solution of 1,2-di(hexyl)etan-1,2-dione **4** (230 mg, 1.01 mmol, 1.0 eq) in acetic acid (5 mL), under inert atmosphere, was added **2** (269 mg, 1.01 mmol, 1.0 eq), the resulting mixture was heated to 90°C and stirred for 16 h. The mixture was cooled to room temperature and then was extracted with EtOAc (5 × 2 mL). The organic phase was washed with $H_2O$ (10 × 2 mL) and dried on anhydrous $Na_2SO_4$. The solvents were evaporated under vacuum. The crude product was purified by flash chromatography ($SiO_2$, petroleum ether / DCM 3:1), obtaining the product **6** as a pale white solid (180 mg, 0.39 mmol, 39%). $^{1}$H-NMR (400 MHz, $CDCl_3$): δ = 7.81 (s, 2H); 3.07 (t, *J* = 9.4 Hz, 4H), 1.80-2.00 (m, 4H); 1.35-1.50 (m, 12 H); 0.89-0.91 (m, 6H) ppm. $^{13}$C-NMR (100 MHz, $CDCl_3$): δ = 158.4, 139.4, 132.1, 123.5, 34.9, 31.9, 29.3, 27.9, 22.8, 14.3 ppm. ESI-MS: *m/z* = 458.05 456.32, 454.06 (1:2:1) $[M+H]^+$.

*10-(4-(4,4,5,5-tetramethyl-1,3,2-dioxaborolan-2-yl)phenyl)-10H-phenothiazine (**9**)*

In a Schlenk tube, under a nitrogen atmosphere, a solution of $Pd_2(dba)_3{\cdot}CHCl_3$ (52 mg, 0.05 mmol, 0.05 eq) in dry toluene (10 mL) was prepared. Then, Xantphos (58 mg, 0.1 mmol, 0.1 eq) was added and the solution stirred for 20'. Phenothiazine (200 mg, 1.0 mmol, 1.0 eq), 1-bromo-4-iodo-benzene (311 mg, 1.1 mmol, 1.1 eq) and NaO$^t$Bu (288 mg, 3.0 mmol, 3.0 eq) were added to the mixture and the latter was heated at 90°C for 24 h. The mixture was then filtrated on Celite®. The filtrate was diluted with EtOAc (20 mL) and washed with $H_2O$ (10 mL) and brine (10 mL). The organic phase was

dried on $Na_2SO_4$ and the solvent was removed under reduced pressure. The crude product was purified by flash column chromatography ($SiO_2$, petroleum ether / DCM 6:1) to give 10-(4-bromophenyl)-10H-phenothiazine as a a white solid (350 mg, 99%). $^1$H-NMR (200 MHz, $CDCl_3$): δ = 7.72 (d, J = 8.2 Hz, 2H), 7.25 (d, J = 8.4 Hz, 2H), 7.08 (dd, J = 7.0, 2.0 Hz, 2H), 6.75-6.90 (m, 4H), 6.24 (dd, J = 7.2, 1.8 Hz, 2H) ppm. Spectroscopic data are in agreement with those reported in literature.[3]

In a Schlenk tube, the product of the previous reaction (350 mg, 0.988 mmol, 1.0 eq) was dissolved in dry THF (8 mL), and *bis*-pinacolatodiboron (501 mg, 1.97 mmol,2.0 eq), Pd(dppf)$Cl_2$ (81 mg, 0.099 mmol,0.1 eq) and AcOK (291 mg, 2.96 mmol,3.0 eq) were added to the solution, which was then kept under stirring at room temperature. After 24 h the reaction mixture was diluted with EtOAc (20mL) and washed with $H_2O$ (10 mL) and brine (10 mL). The organic phase was dried on $Na_2SO_4$ and the solvents removed under reduced pressure. The crude product was purified by flash column chromatography ($SiO_2$, petroleum ether / DCM 3:1), giving product **9** as a white solid (234 mg, 59%). $^1$H-NMR (200 MHz, $CDCl_3$): δ = 7.63 (d, J= 8.0 Hz, 2H), 7.28 (d, J = 8.2 Hz, 2H), 7.08 (dd, J = 7.0, 2.0 Hz, 2H), 6.75-6.90 (m, 4H), 6.24 (dd, J = 7.2, 1.8 Hz, 2H), 1.65 (s, 12) ppm. Spectroscopic data are in agreement with those reported in literature.[4]

## 2. Computational analysis

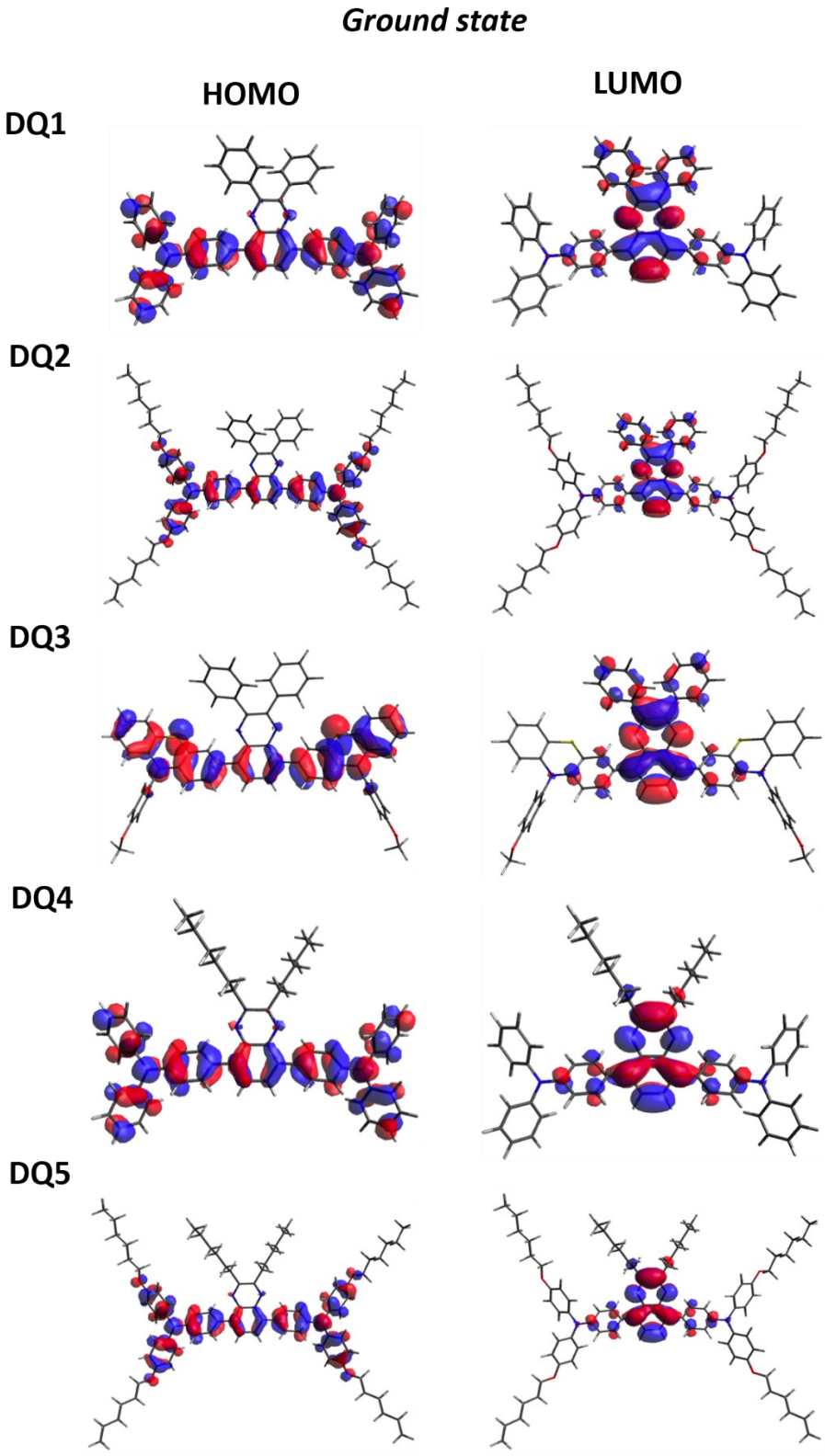


**Figure S1.** Ground-state frontier molecular orbitals (HOMO and LUMO) of compounds **DQs** computed at the B3LYP/6-31G* level**.**

## 3. Spectroscopic analysis at different concentrations in toluene

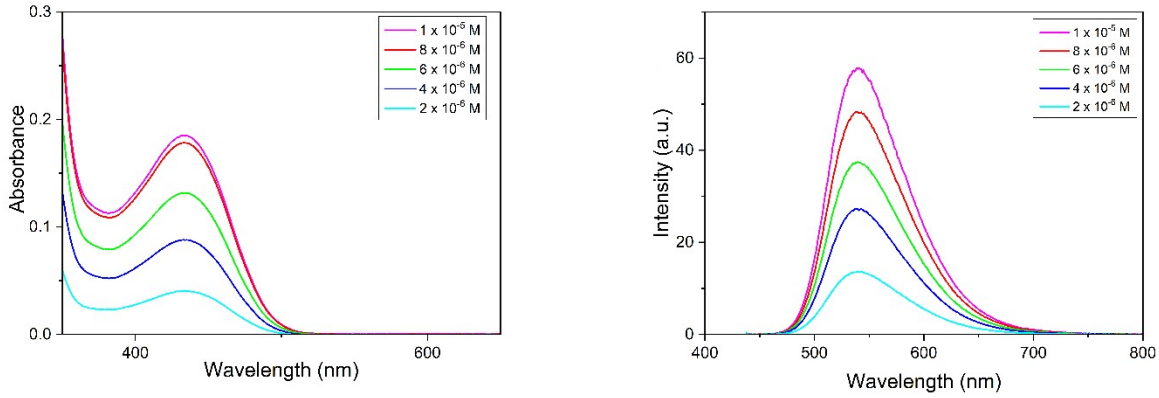


**Figure S2. DQ1** absorbance (on the left) and emission spectra at 433 nm excitation wavelength (on the right), in toluene at different concentrations.

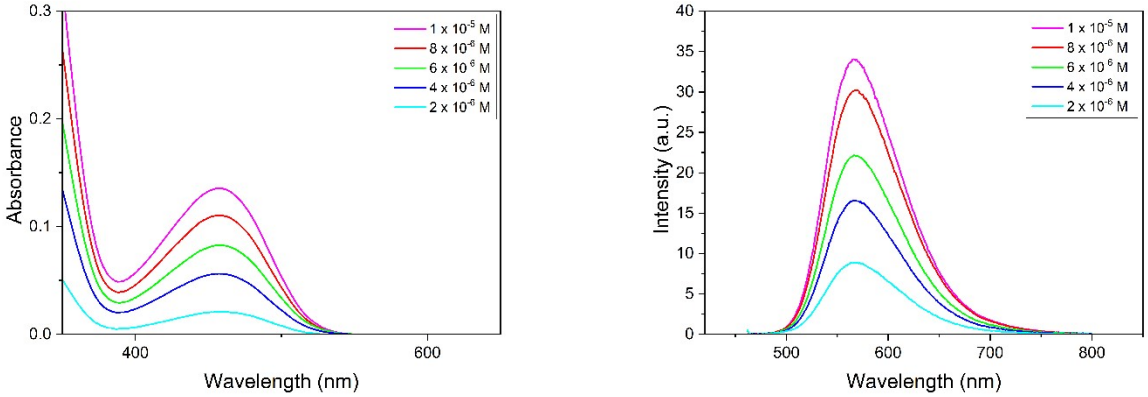


**Figure S3. DQ2** absorbance (on the left) and emission spectra at 457 nm excitation wavelength (on the right), in toluene at different concentrations.

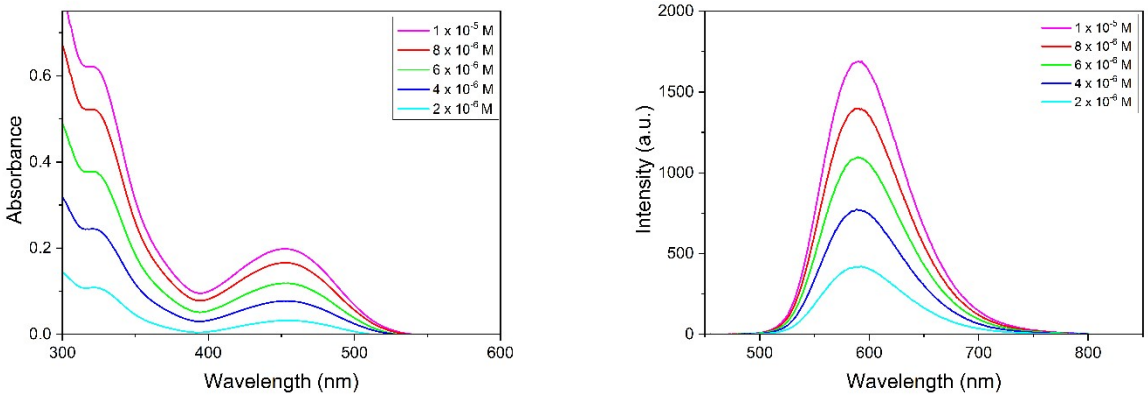


**Figure S4. DQ3** absorbance (on the left) and emission spectra at 452 nm excitation wavelength (on the right), in toluene at different concentrations.

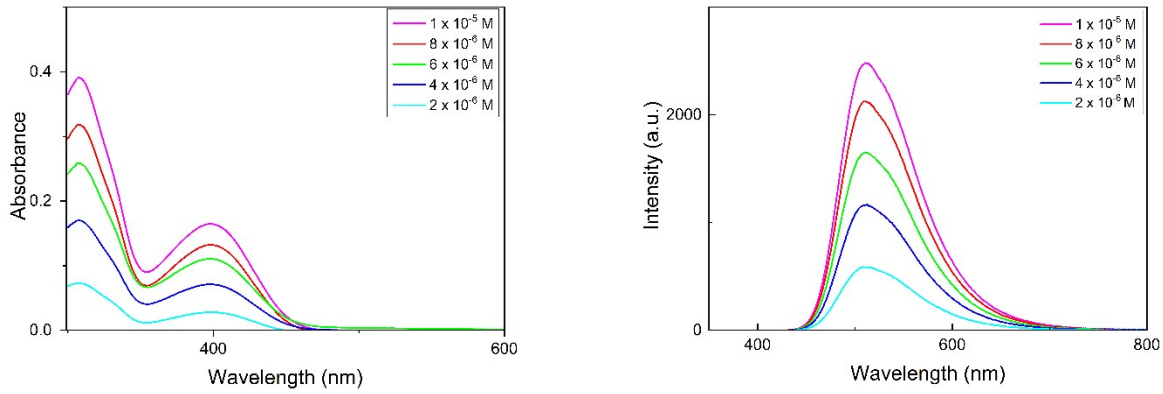


**Figure S5. DQ4** absorbance (on the left) and emission spectra at 398 nm excitation wavelength (on the right), in toluene at different concentrations.

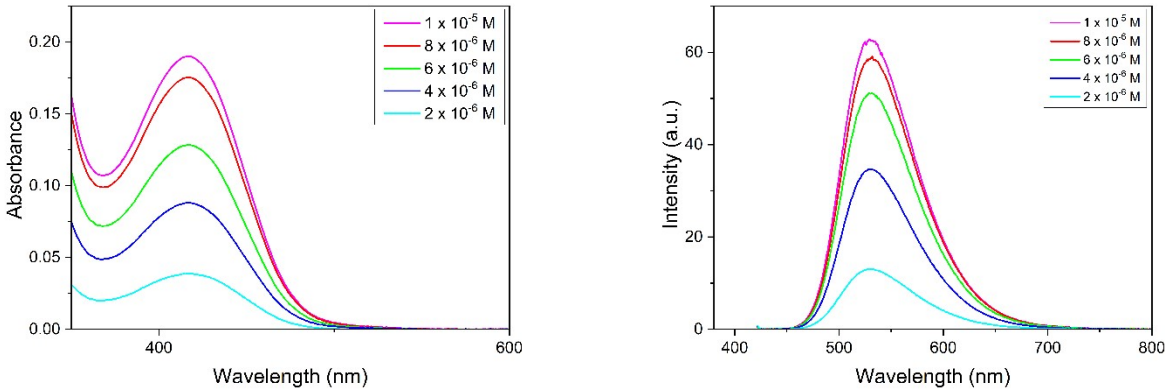


**Figure S6. DQ5** absorbance (on the left) and emission spectra at 416 nm excitation wavelength (on the right), in toluene at different concentrations.

## 4. Spectroscopic analysis at different concentrations in PMMA

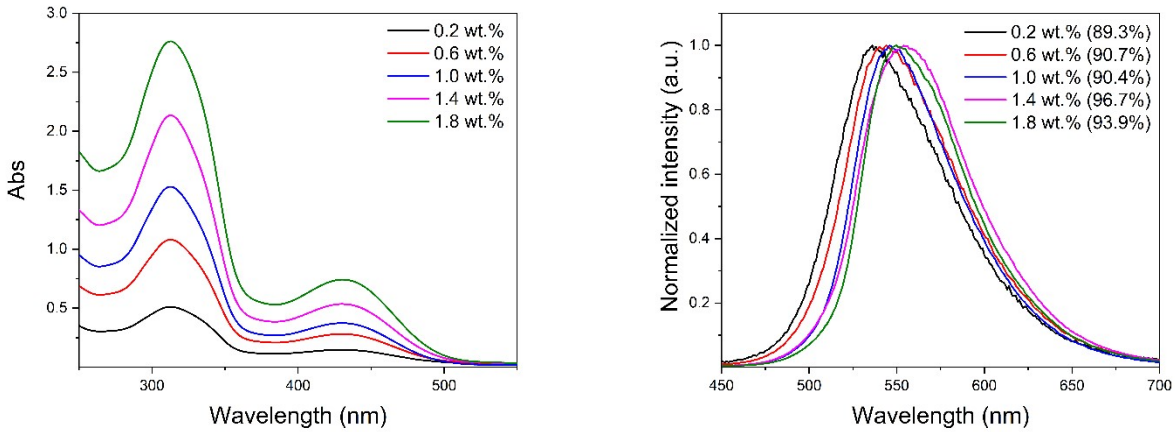


**Figure S7.** UV-Vis absorption spectra as function of fluorophore concentration (wt.%) for **DQ1/**PMMA films (left). Fluorescence spectra (right) of the same films ($\Phi_f$ is reported in parentheses) with an excitation wavelength of 430 nm.

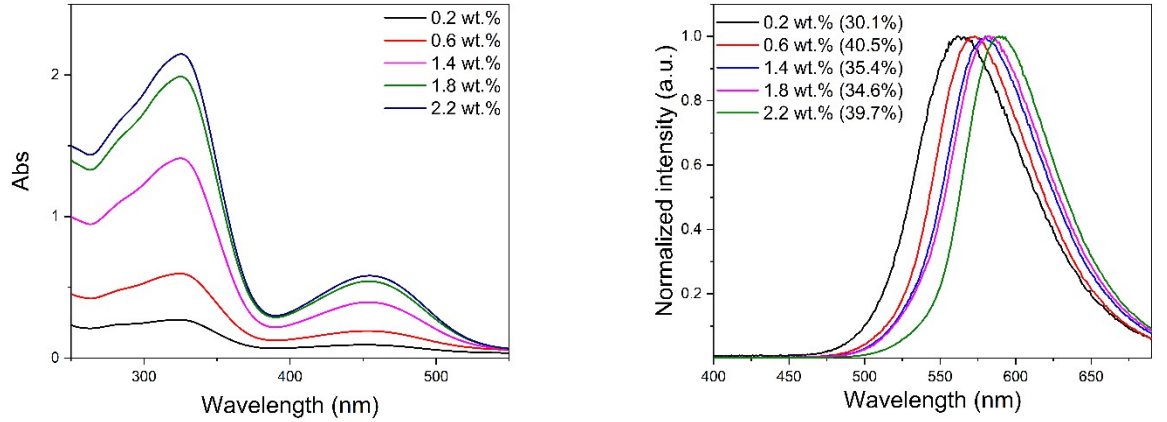


**Figure S8.** UV-Vis absorption spectra as function of fluorophore concentration (wt.%) for **DQ2/**PMMA films (left). Fluorescence spectra (right) of the same films ($\Phi_f$ is reported in parentheses) with an excitation wavelength of 454 nm.

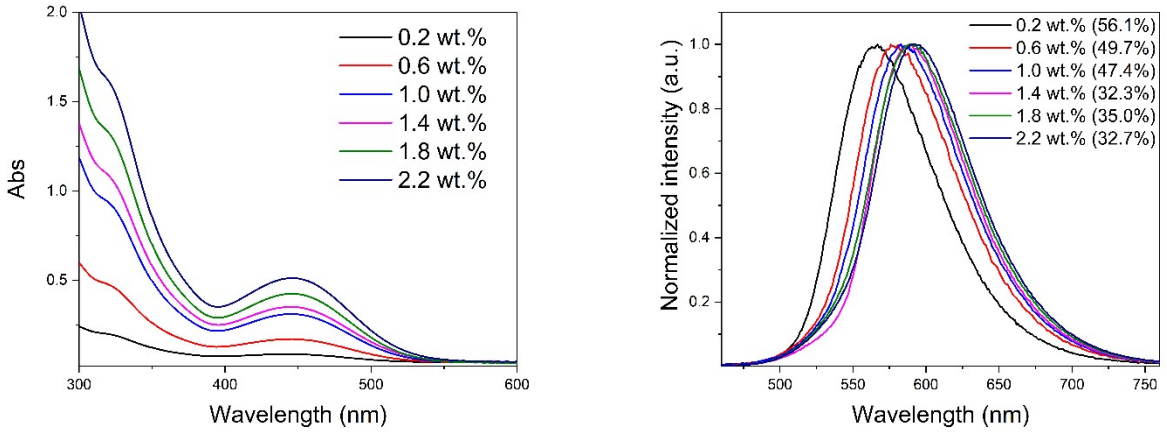


**Figure S9.** UV-Vis absorption spectra as function of fluorophore concentration (wt.%) for **DQ3/**PMMA films (left). Fluorescence spectra (right) of the same films ($\Phi_f$ is reported in parentheses) with an excitation wavelength of 456 nm.

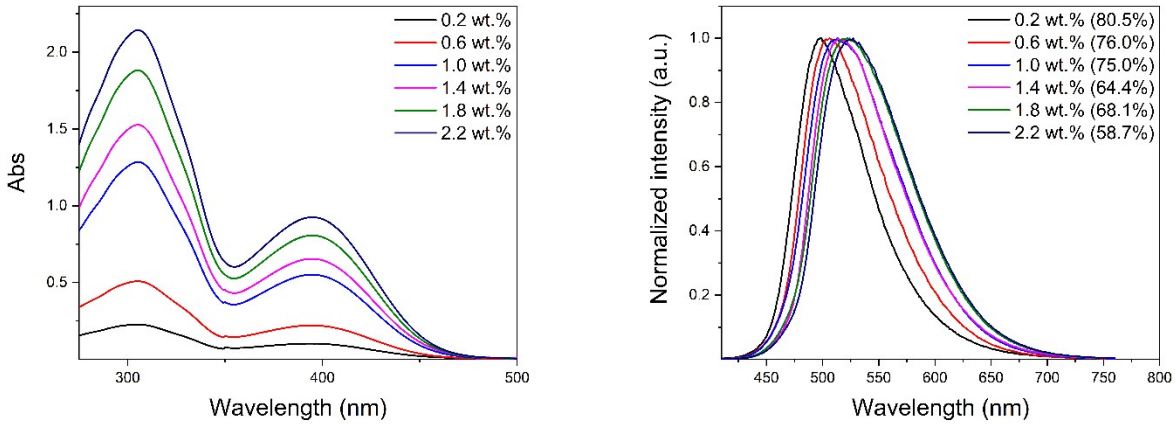


**Figure S10.** UV-Vis absorption spectra as function of fluorophore concentration (wt.%) for **DQ4/**PMMA films (left). Fluorescence spectra (right) of the same films ($\Phi_f$ is reported in parentheses) with an excitation wavelength of 400 nm.

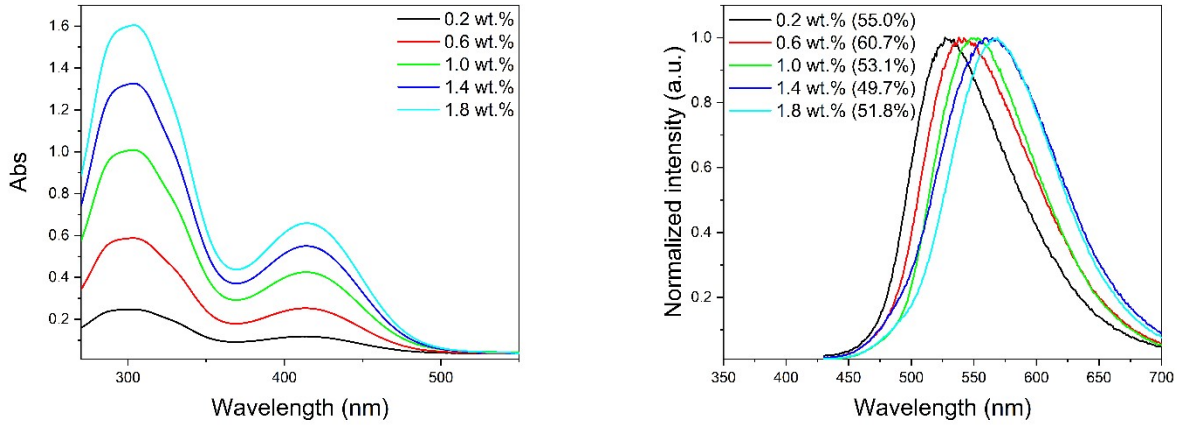


**Figure S11.** UV-Vis absorption spectra as function of fluorophore concentration (wt.%) for **DQ5/**PMMA films (left). Fluorescence spectra (right) of the same films ($\Phi_f$ is reported in parentheses) with an excitation wavelength of 415 nm.

## 5. Spectroscopic analysis at different concentrations in PCMA

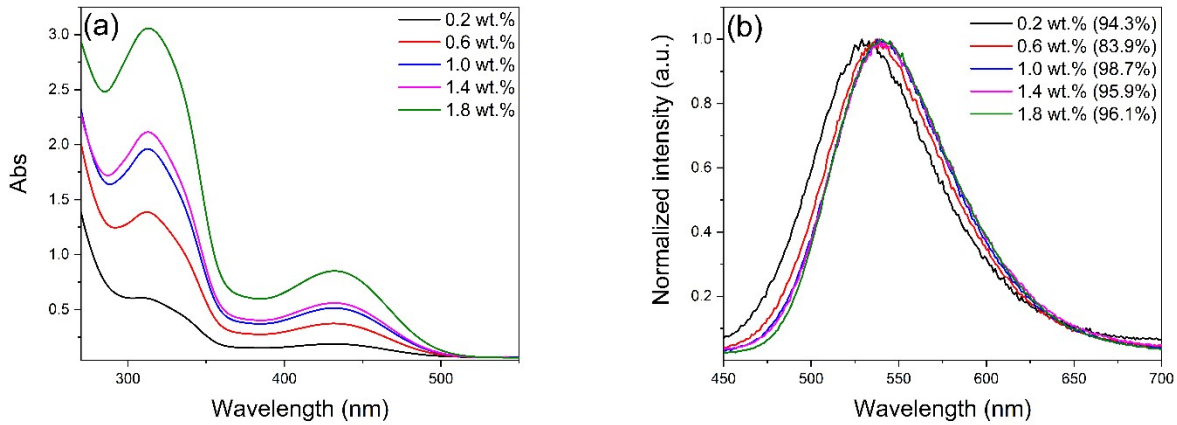


**Figure S12.** UV-Vis absorption spectra as function of fluorophore concentration (wt.%) for **DQ1/**PCMA films (left). Fluorescence spectra (right) of the same films ($\Phi_f$ is reported in parentheses) with an excitation wavelength of 430 nm.

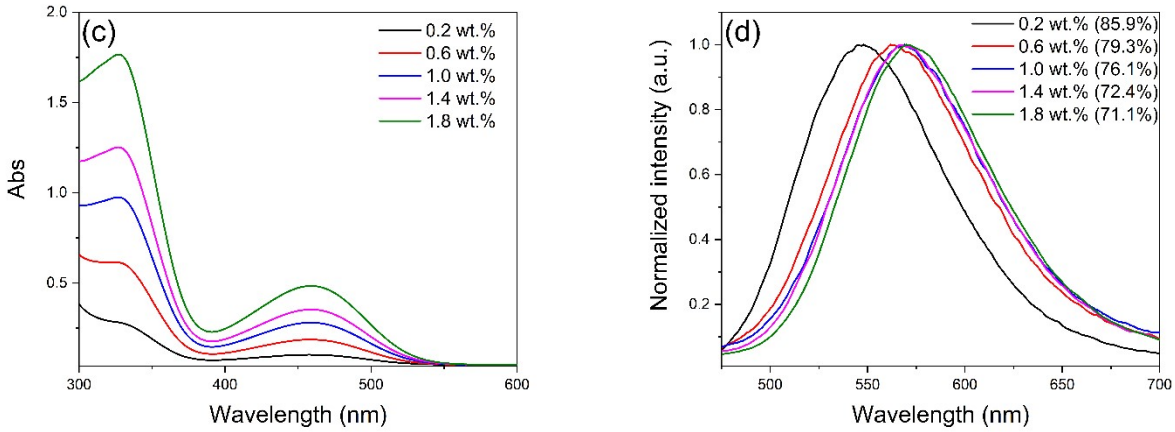


**Figure S13.** UV-Vis absorption spectra as function of fluorophore concentration (wt.%) for **DQ2/**PCMA films (left). Fluorescence spectra (right) of the same films ($\Phi_f$ is reported in parentheses) with an excitation wavelength of 459 nm.

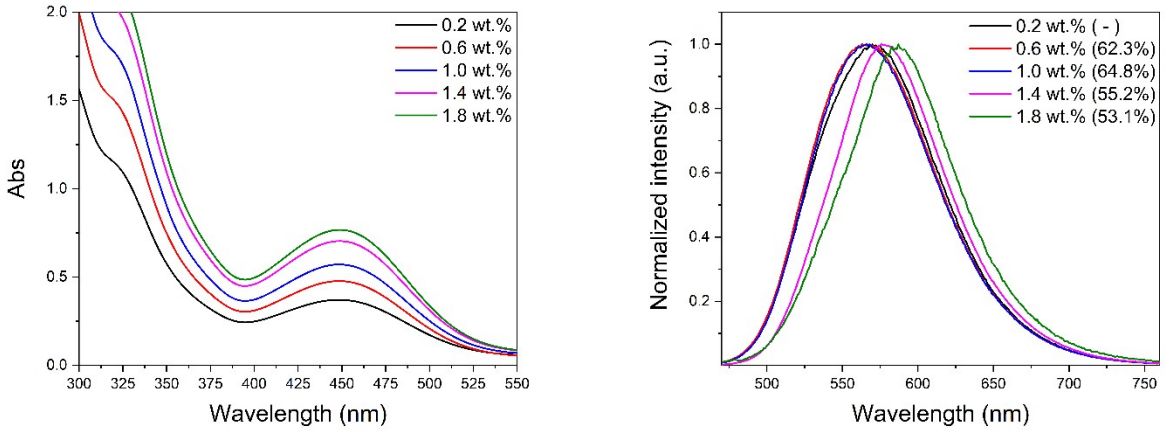


**Figure S14.** UV-Vis absorption spectra as function of fluorophore concentration (wt.%) for **DQ3/**PCMA films (left). Fluorescence spectra (right) of the same films ($\Phi_f$ is reported in parentheses) with an excitation wavelength of 447 nm.

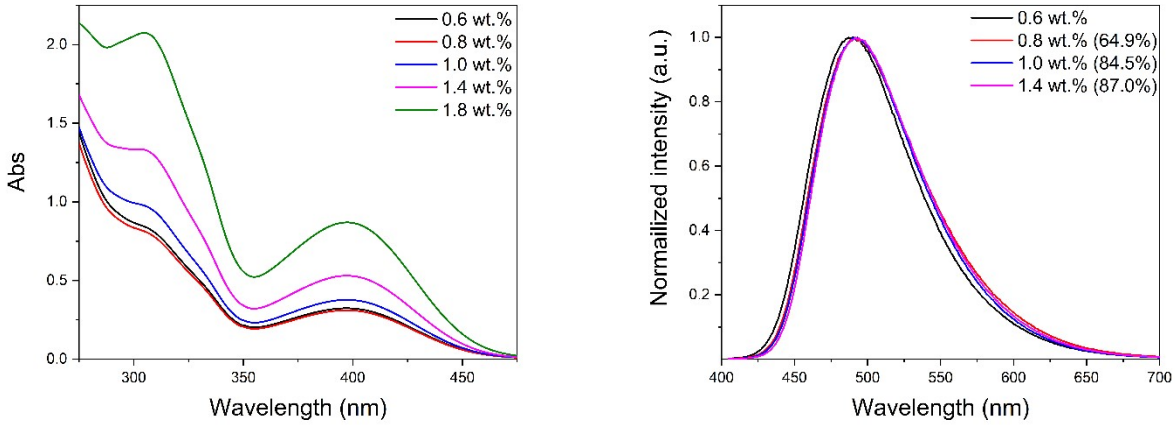


**Figure S15.** UV-Vis absorption spectra as function of fluorophore concentration (wt.%) for **DQ4/**PCMA films (left). Fluorescence spectra (right) of the same films ($\Phi_f$ is reported in parentheses) with an excitation wavelength of 400 nm.

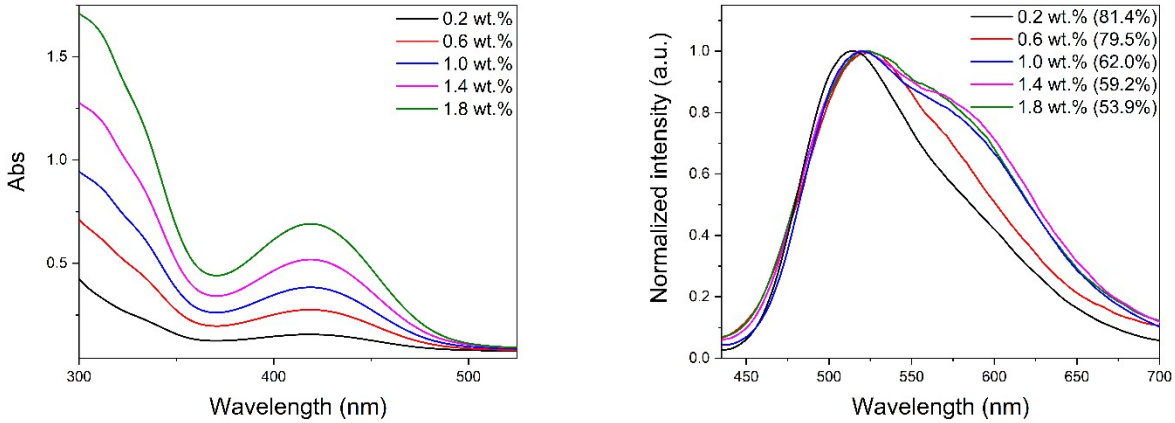


**Figure S16.** UV-Vis absorption spectra as function of fluorophore concentration (wt.%) for **DQ5/**PCMA films (left). Fluorescence spectra (right) of the same films ($\Phi_f$ is reported in parentheses) with an excitation wavelength of 419 nm.

## 6. Further Time Resolved Spectra

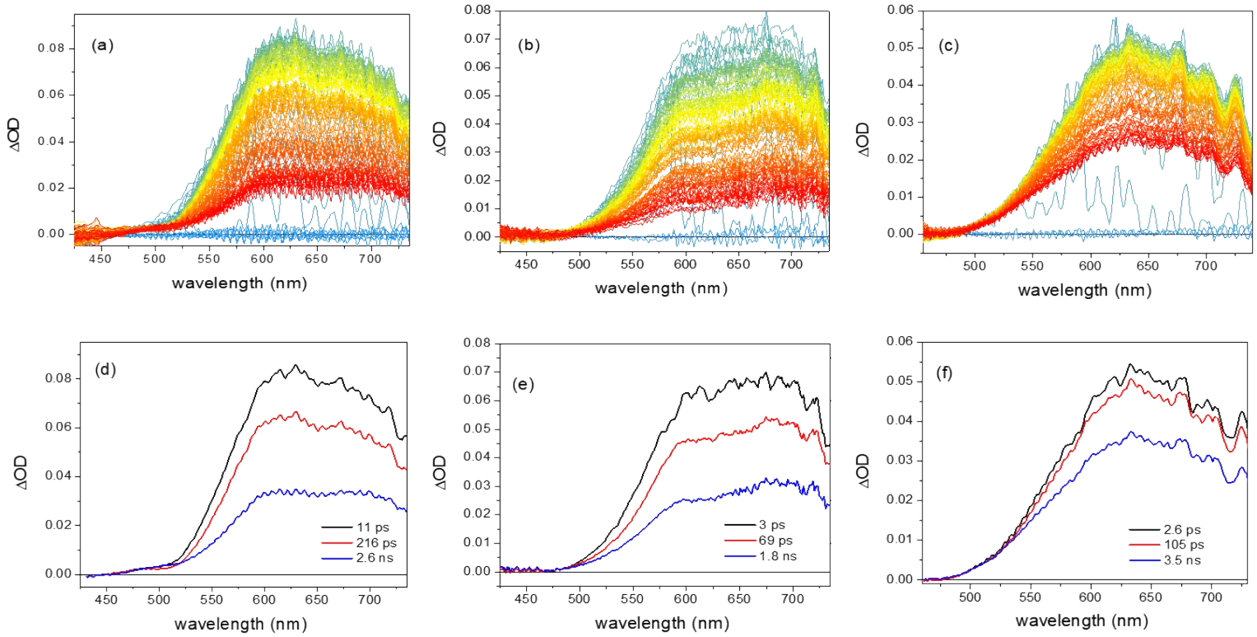


**Figure S17**. Transient absorption spectra (a, b, c) and relative Evolution Associated Difference Spectra (d,e,f) of respectively **DQ1**, **DQ2** and **DQ3** in PMMA (1%wt concentration).

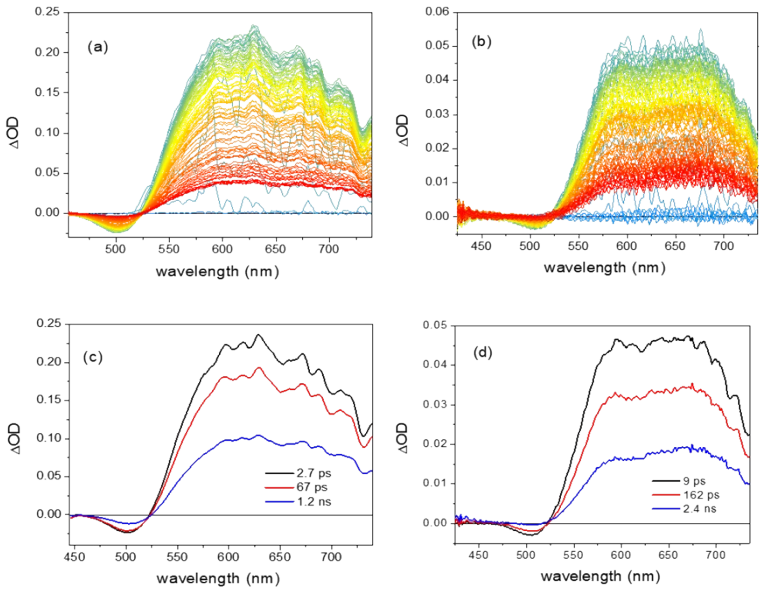


**Figure S18.1**. Transient absorption spectra (a, b) and relative Evolution Associated Difference Spectra (d,e) of respectively **DQ4**, and **DQ5** in PMMA (1%wt concentration).

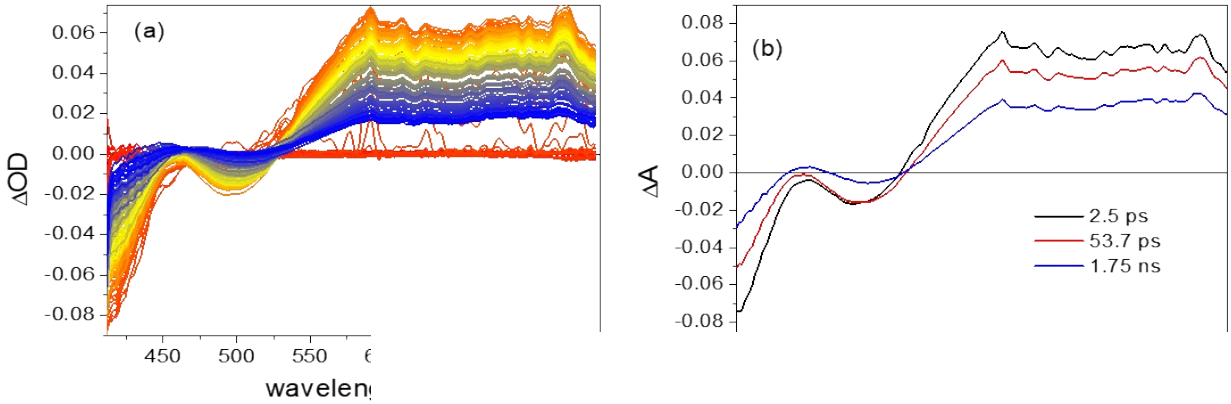


**Figure S18.2**: Transient absorp
dispersed in PCMA (excitation

## 7. Copies of the NMR sp

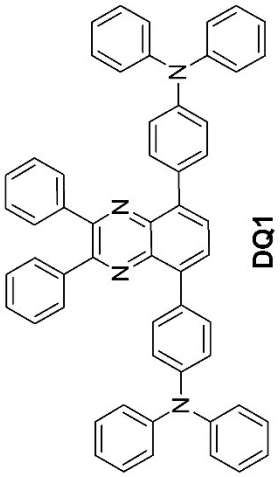


DQ1

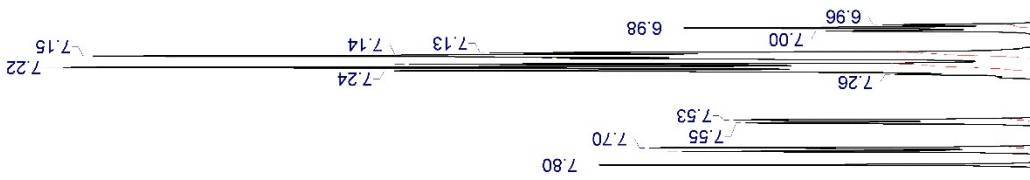

77.32
77.00
76.68
122.73
122.96
124.67
128.13
129.24
131.68
132.11
138.53
139.11
147.32
147.71
150.97
N
N
N
N
DQ1

0.91
0.90
0.93
0.85
0.87
1.55
1.35
1.36
1.37
1.47
1.26
1.78
1.76
1.74
1.79
3.95
3.93
3.97
5.32
6.88
6.85
7.84
7.69
7.67
7.56
7.35
7.33
7.31
7.14
7.12
7.04
DQ2

14.38
23.19
26.27
29.86
32.16
53.46
53.73
54.00
54.27
54.54
68.83
115.76
119.47
127.60
130.35
130.42
131.90
138.85
139.81
141.02
148.96
151.63
156.34
DQ2

3.92
6.00
6.19
6.19
6.21
6.21
6.29
6.31
6.80
6.82
6.82
6.79
6.86
7.02
7.03
7.14
7.16
7.26
7.32
7.36
7.38
7.59
7.59
7.61
7.75
1.82
1.57
3.69
4.08
7.41
4.09
1.86
4.17
1.89
1.86
DQ3

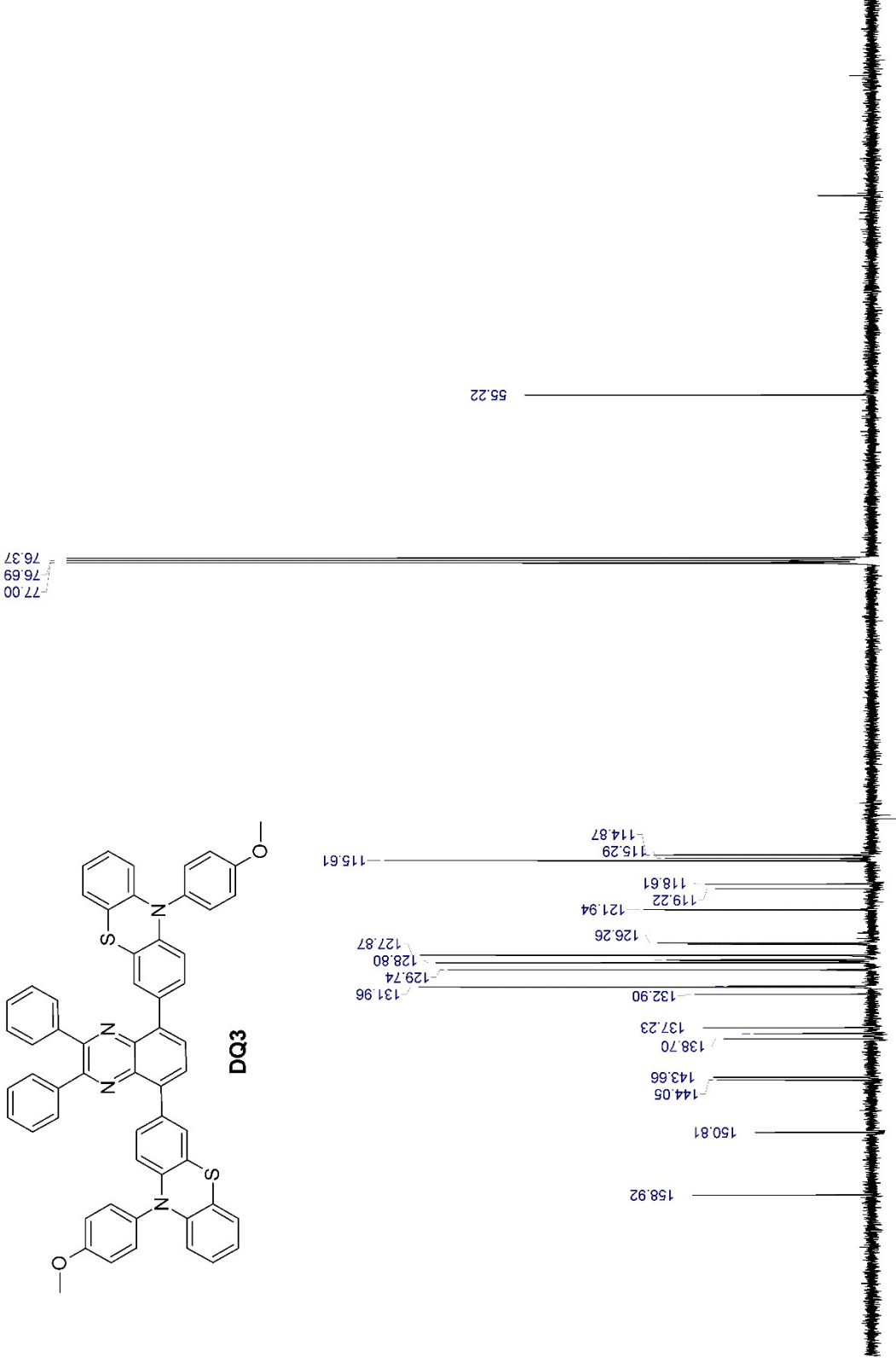
55.22
77.00
76.69
76.37
158.92
150.81
144.05
143.66
138.70
137.23
132.90
131.96
129.74
128.80
127.87
126.26
121.94
119.22
118.61
115.61
115.29
114.87
DQ3

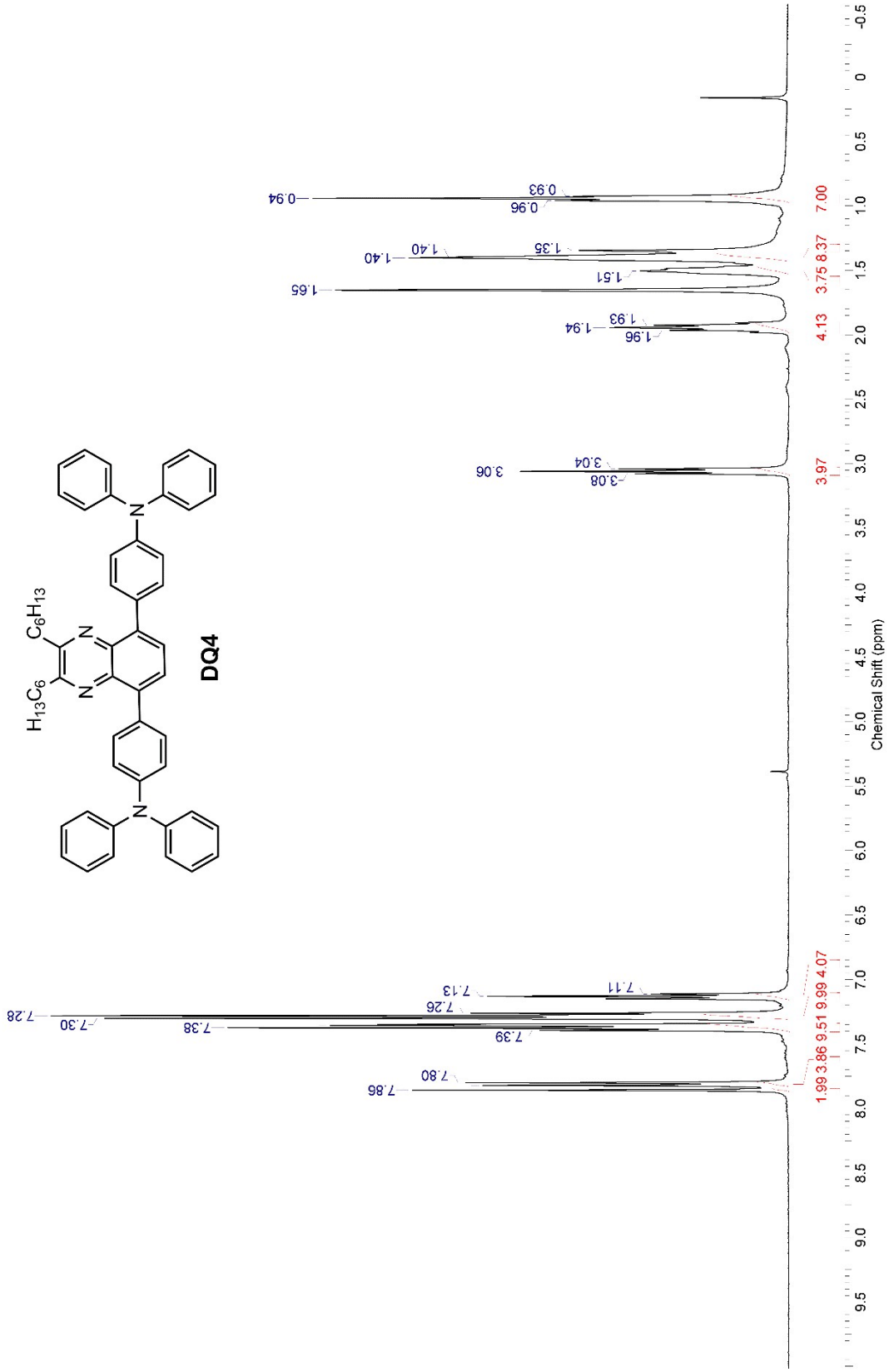
DQ4
Chemical Shift (ppm)

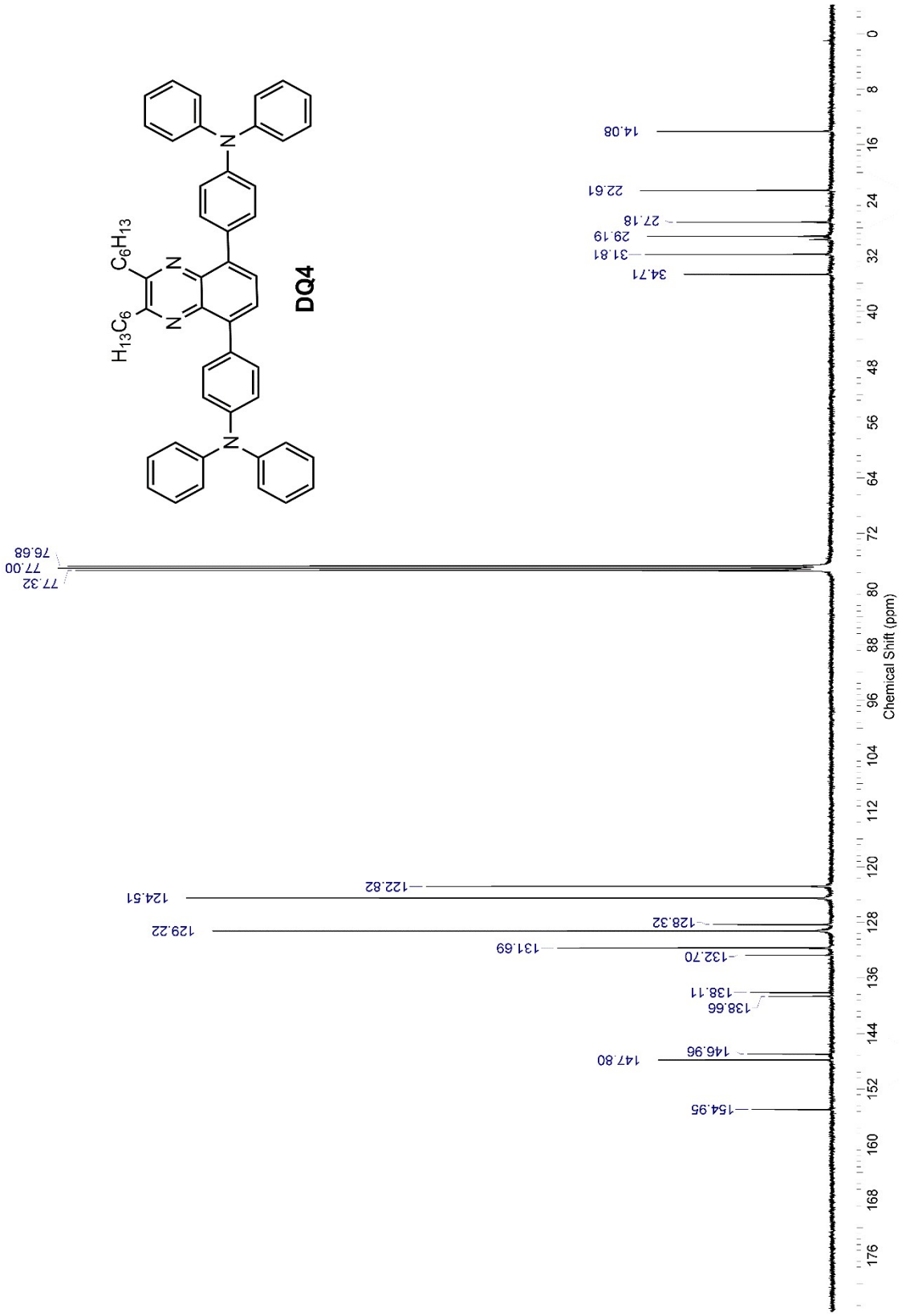
DQ4
$C_6H_{13}$
$H_{13}C_6$
N
14.08
22.61
27.18
29.19
31.81
34.71
76.68
77.00
77.32
122.82
124.51
128.32
129.22
131.69
132.70
138.11
138.66
146.96
147.80
154.95
Chemical Shift (ppm)

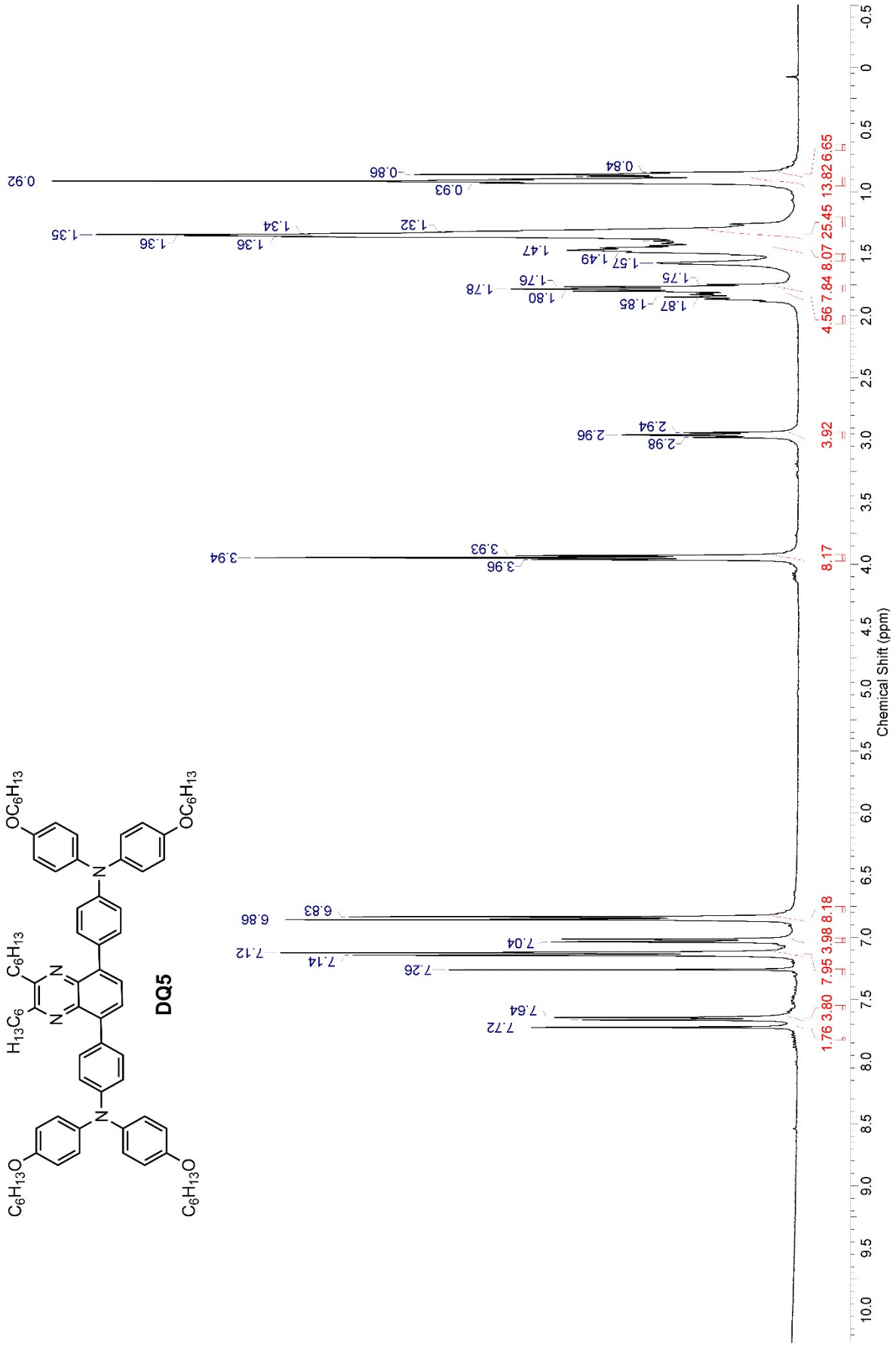
DQ5
Chemical Shift (ppm)

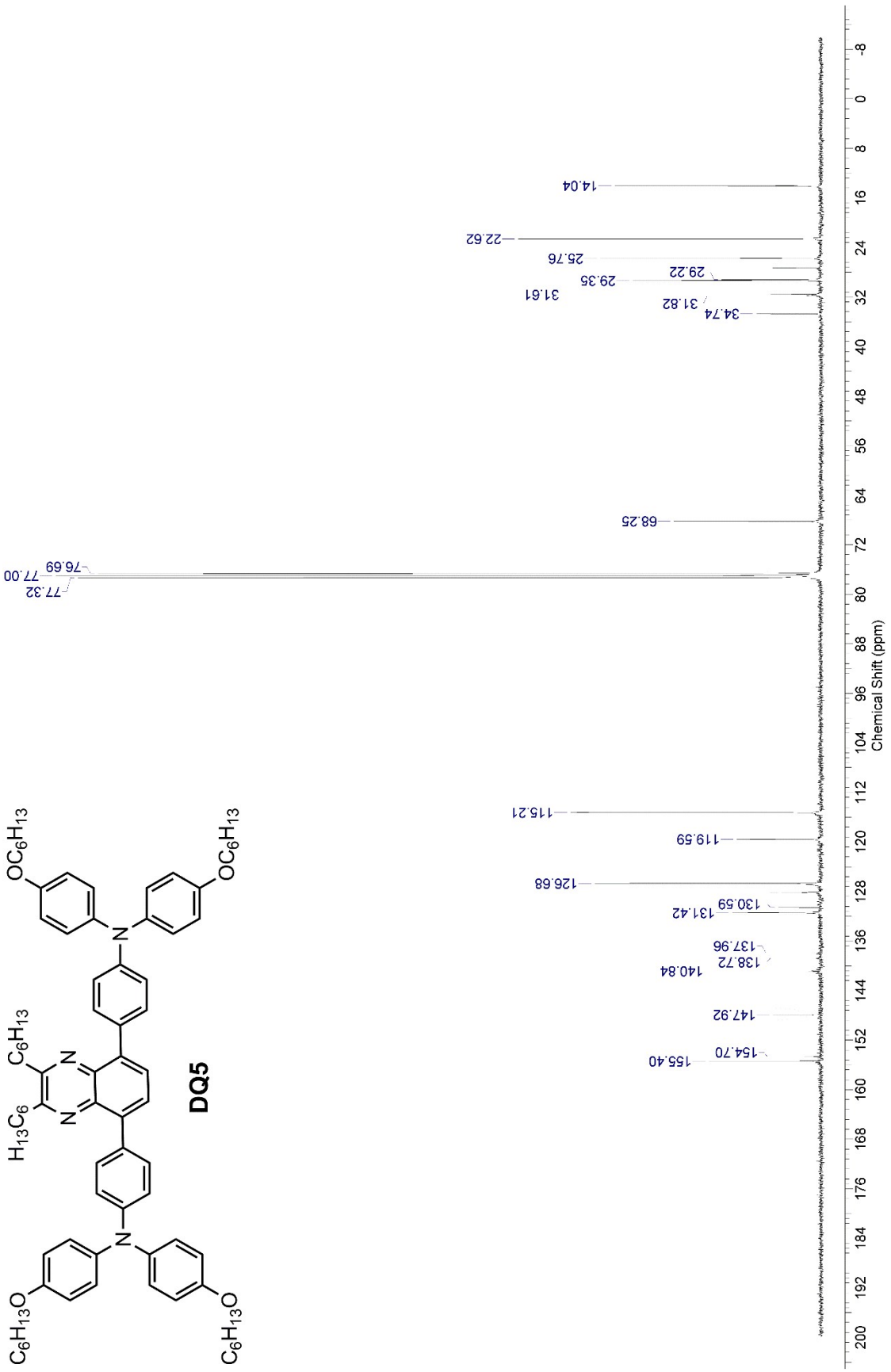
DQ5
Chemical Shift (ppm)
14.04
22.62
25.76
29.22
29.35
31.61
31.82
34.74
68.25
76.69
77.00
77.32
115.21
119.59
126.68
130.59
131.42
137.96
138.72
140.84
147.92
154.70
155.40

## 8. Fluorescence lifetimes of compounds DQ1-5 in PMMA matrix

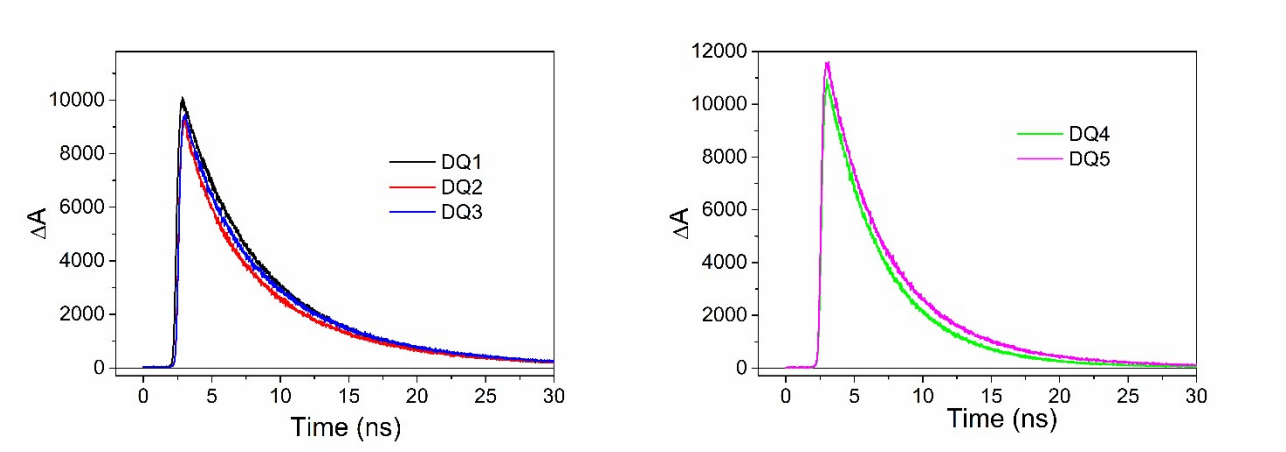


***Figure S19.*** *Fluorescence decay profiles measured for the different compounds in PMMA at 1.0 wt% concentration.*

***Table S1.*** Fluorescence lifetimes obtained with a bi-exponential fit of the curves reported in Fig.S32. Values are obtained as the average fit of three independent measurements for each sample.

| Compound | $\tau_1$ (ns) | $A_1$ | $\tau_r$ (ns) | $A_2$ | $X^2$ |
|---|---|---|---|---|---|
| **DQ1** | 7.8 | 3068.3 (40.4%) | 4.2 | 4526.3 (59.6%) | 1.014 |
| **DQ2** | 7.9 | 5506.0 (57.4 %) | 2.7 | 4087.7 (42.6%) | 1.09 |
| **DQ3** | 8.1 | 5804.3 (61.9%) | 2.8 | 3570.0 (38.1%) | 1.082 |
| **DQ4** | 6.3 | 2349.0 (20.5%) | 3.7 | 9134.7 (79.5%) | 1.093 |
| **DQ5** | 6.7 | 5273.3 (39.5%) | 3.4 | 8091.7 (60.5%) | 1.07 |

## 9. Determination of LSC performances.

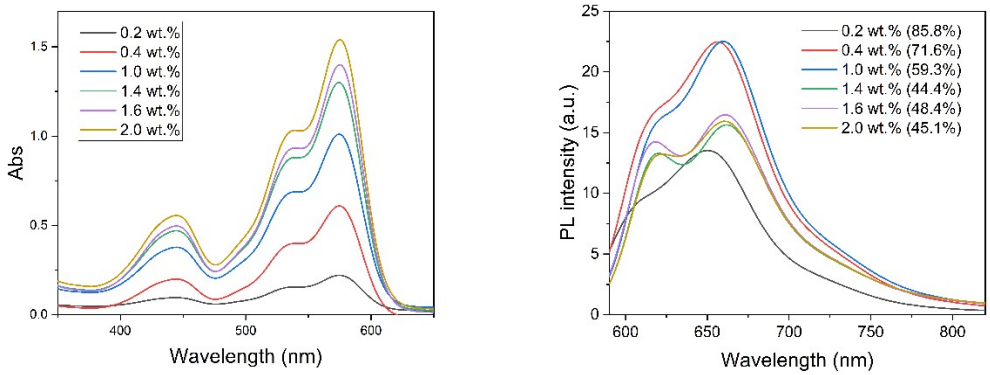


**Figure S20.** *Spectroscopic analysis of reference fluorophore **LR305**/PMMA: absorbance (on the left) and emission spectra at 575 nm excitation wavelength (on the right), at different concentrations. ($\Phi_f$ is reported in parentheses).*

**Edge-emitted power as a function of distance of the excitation spot from the edge**

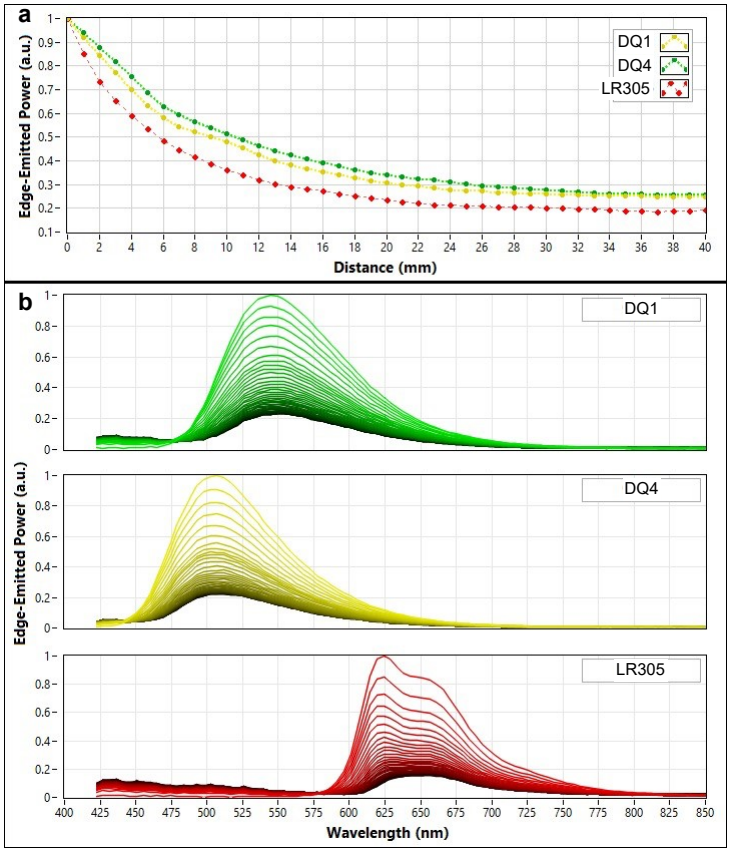


**Figure S21.** a) Normalized edge-emitted power and b) emission spectra recorded as a function of the optical pathlength distance between the excitation spot ($\lambda_{exc}$ = 405 nm, 35 W/cm$^2$) and the collecting edge.

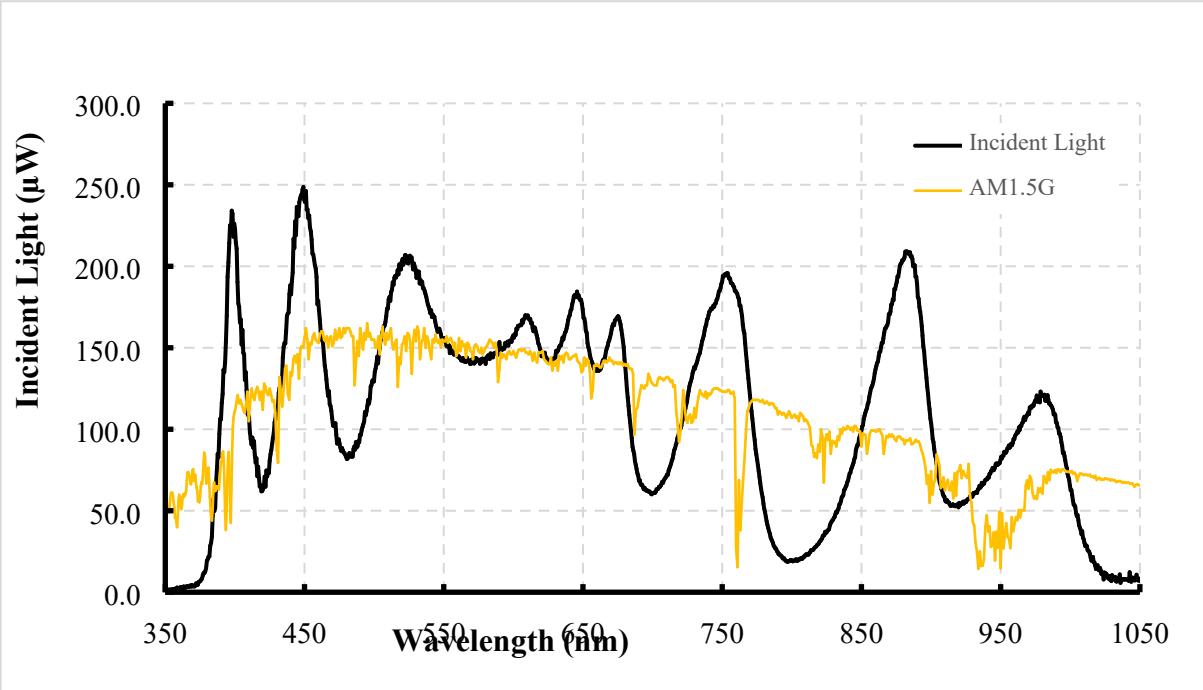


***Figure S22.*** *Spectra of the incident light generated by a custom LED tower containing 12 LEDs (black line, used for the internal and the external photon efficiency measures) and of the AM1.5G (yellow line).*

**Evaluation of internal photon efficiency ($\eta_{int}$) and external photon efficiency ($\eta_{ext}$)**

All the measurements were performed by using a commercially available system (Arkeo – Cicci research s.r.l.) containing a CMOS-based spectrometer with a symmetrical Czerny-Turner optical bench connected to an integrating sphere (Figure S22).

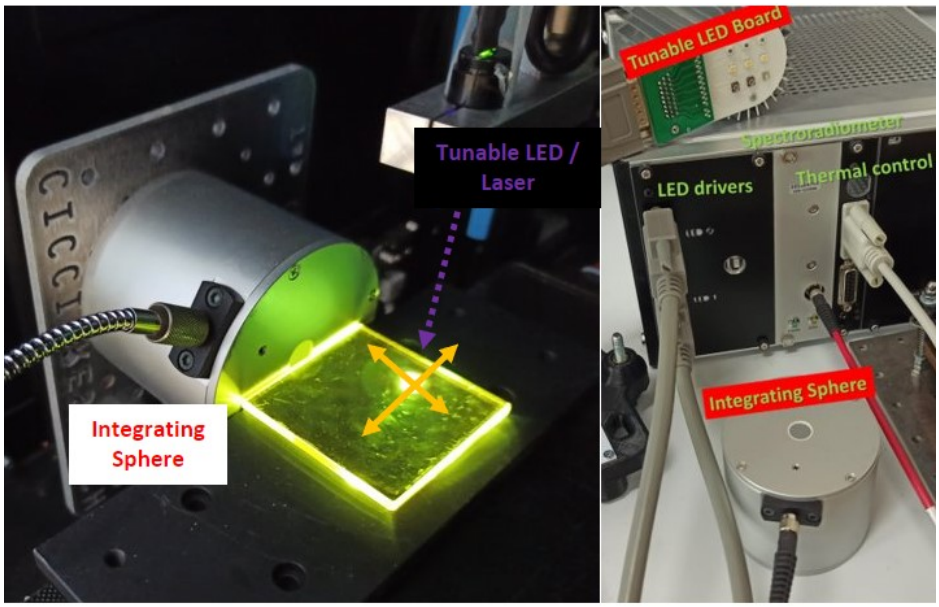


**Figure S23.** Photos of the experimental setup utilized for the $\eta_{int}$ and $\eta_{ext}$ determination

A fiber based tunable LED source was used to excite the center of the LSC device with a circular spot of 2 mm of diameter. The platform includes a tunable LED source composed by 10 monochromatic diodes (from 360 to 960 nm) and 2 white diodes (warm and cold) used to match AM 1.5G (Fig, S21). The use of LED source allowed the irradiation stability with time. An integrating sphere of 5 cm of diameter and 1 cm of aperture is placed along the edge of the glass plate, such that the aperture of the sphere is fully covered by the glass and one corner coincides with the edge of the aperture hole. The integrating sphere was moved along the side of the LSC until all the slab edge had been scanned. The spectrally-resolved edge output photon count was collected from the CMOS-based spectrometer and calibrated into optical power (W) and then in irradiance. Aimed at limiting reflections of unabsorbed light, an absorbing matte black background was placed in contact with the LSC rear side. The fiber was kept close and perpendicular to the center of the LSC front surface to minimize the diverge of the excitation beam and to avoid the direct illumination of the integrating sphere[5]. A series of 3-5 measurements were repeated in order align the integration sphere to collect the maximum single-edge output power.

The optical performances of LSC based on **LR305**, **DQ1** and **DQ4** were evaluated in terms of the internal and the external photon efficiency ($\eta_{int}$ and $\eta_{ext}$, respectively). $\eta_{int}$ and $\eta_{ext}$ were obtained according to recently published protocols,[6,7]] and were calculated from the equations S1 and S2:

$$\eta_{int} = \frac{\text{no. of edge} - \text{emitted photons}}{\text{no. of total absorbed photons}} = \frac{\sum_{i=1}^{i=n}\int_{\lambda_1}^{\lambda_2} P_{out,i}(\lambda)\frac{\lambda}{hc}d\lambda}{\int_{\lambda_1}^{\lambda_2} P_{abs}(\lambda)\frac{\lambda}{hc}d\lambda} = \frac{\sum_{i=1}^{i=n}\int_{\lambda_1}^{\lambda_2} P_{out,i}(\lambda)\frac{\lambda}{hc}d\lambda}{\int_{\lambda_1}^{\lambda_2} P_{in}(\lambda)(1-10^{-A(\lambda)})\frac{\lambda}{hc}d\lambda} \quad \text{(Eq. S1)}$$

$$\eta_{ext} = \frac{\text{no. of edge} - \text{emitted photons}}{\text{no. of total incident photons}} = \frac{\sum_{i=1}^{i=n}\int_{\lambda_1}^{\lambda_2} P_{out,i}(\lambda)\frac{\lambda}{hc}d\lambda}{\int_{\lambda_1}^{\lambda_2} P_{in}(\lambda)\frac{\lambda}{hc}d\lambda} \quad \text{(Eq. S2)}$$

Where:

a) n = 4, $\lambda_1$ = 350 nm and $\lambda_2$ = 1050 nm;

b) the number of edge emitted photons were obtained from the sum of the output power spectra measured for each edge of the LSC;

c) the number of total absorbed photons were obtained by convolution of the absorption spectrum of the LSC and the input power spectrum of the light source incident on the illuminated surface area of the LSC. Such value was also obtained by the difference between the incident input power and the transmitted power by the LSC.

d) The total number of photons incident on the front surface of the LSC was obtained from the input power spectrum of the light source incident on the illuminated surface area of the LSC.

***Table S2***. Optical parameters recorded for 5x5 cm² LSC devices.

| LSC | Input Power (μW/cm²) | Absorbed Power (μW/cm²) | Output Power (μW/cm²) | $\eta_{ext}$ | $\eta_{int}$ |
|---|---|---|---|---|---|
| LR305/PMMA | 1874.0 | 525.6 | 87.5 | 4.7 | 16.6 |
| DQ4/PMMA | 1874.0 | 213.6 | 67.0 | 3.6 | 27.9 |
| DQ1/PMMA | 1874.0 | 270.3 | 115.9 | 6.2 | 42.9 |

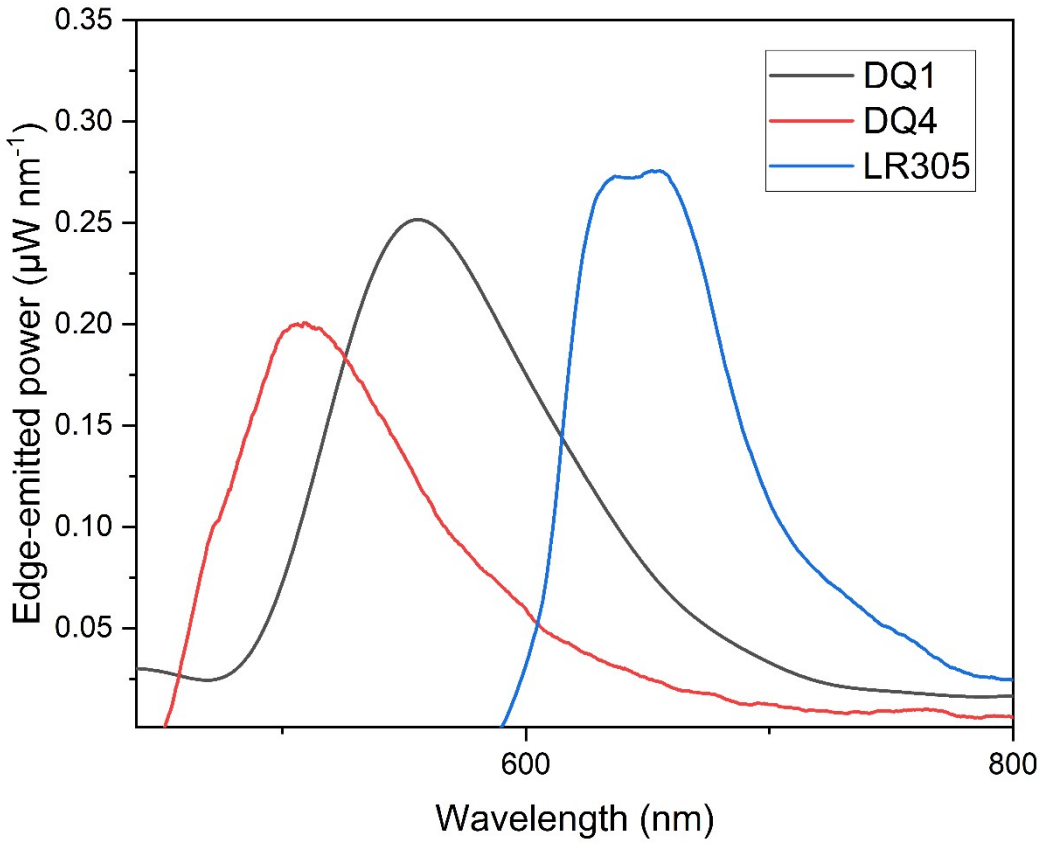


**Figure S24.** Edge emitted power spectra of **DQ1**/PMMA (1.4 wt.%), **DQ4**/PMMA (1.4 wt.%) and **LR305**/PMMA (1.0 wt.%) films-based LSC systems.

## 10. Thermogravimetric analysis of compounds DQ1 and DQ2

Thermogravimetric (TGA) analysis of compounds **DQ1** and **DQ2** was conducted under inert $N_2$ atmosphere with an EXSTAR Seiko 6200 instrument, using the following parameters: temperature range, 30-500 °C; temperature ramp, 10 °C/min; N2 gas flow 100 mL/min.

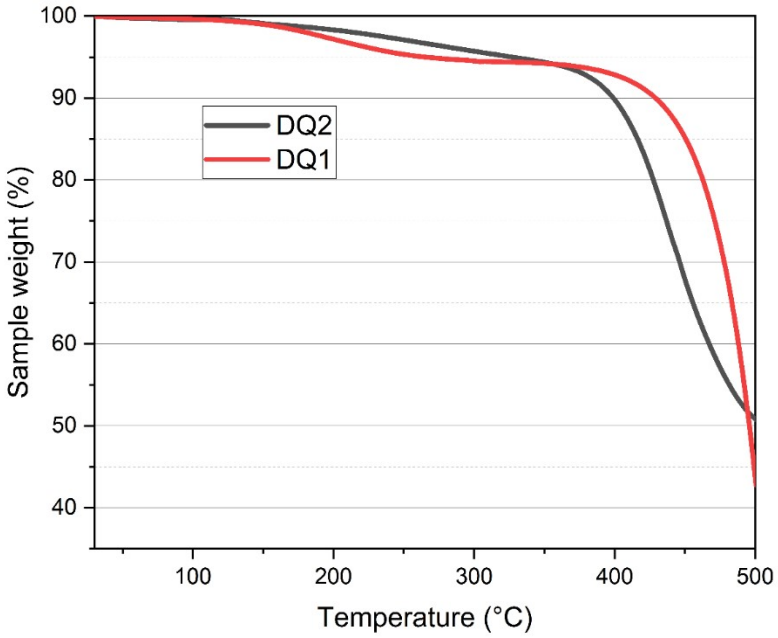


**Figure S25.** *Thermogravimetric analysis of compounds **DQ1** (red line) and **DQ2** (black line).*

**11. Photostability of DQ1/PMMA and LR305/PMMA films.**

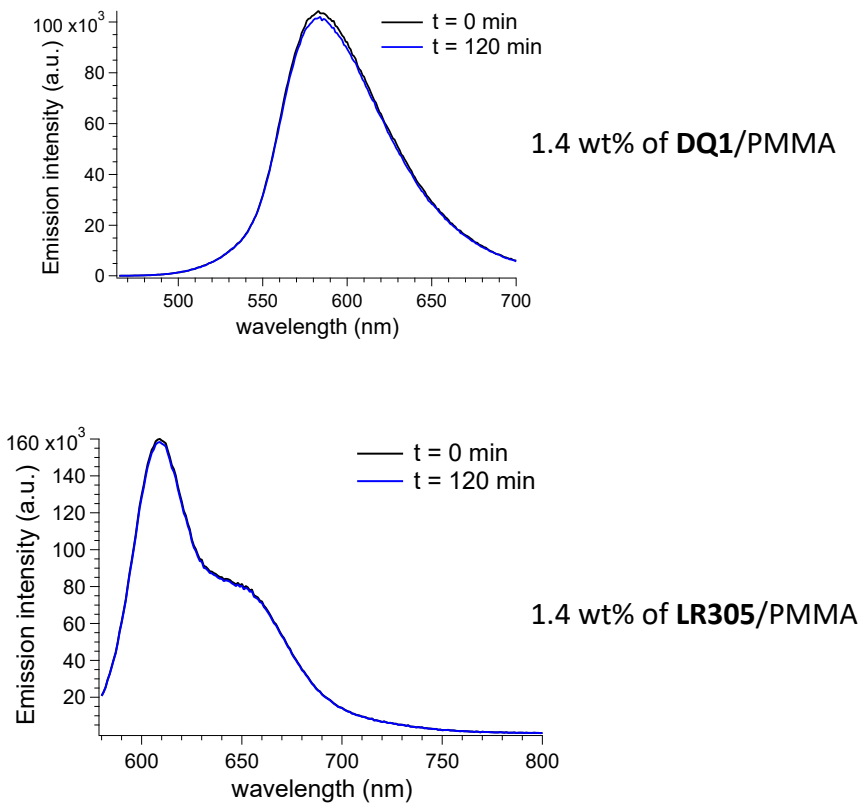


**Figure S26:** Emission profiles of 1.4 wt% of **DQ1**/PMMA (top) and **LR305**/PMMA (bottom) before and after the continuous excitation at the maximum absorption (430 and 575 nm, respectively) for 120 min with a 450 W Xe arc lamp under aerobic conditions and irradiances of about 50 µW/cm$^2$.

## 12. References


1 L. Wang, J. Zhou, Y. Lan, S. Ding, W. Yu and W. Wang, Divergent Synthesis of Chiral Covalent Organic Frameworks, *Angew. Chemie Int. Ed.*, 2019, **58**, 9443–9447.

2 B. Nowacki, H. Oh, C. Zanlorenzi, H. Jee, A. Baev, P. N. Prasad and L. Akcelrud, Design and synthesis of polymers for chiral photonics, *Macromolecules*, 2013, **46**, 7158–7165.

3 C. Liu, Q. Jiang, Y. Lin, Z. Fang and K. Guo, C- To N-Center Remote Heteroaryl Migration via Electrochemical Initiation of N Radical by Organic Catalyst, *Org. Lett.*, 2020, **22**, 795–799.

4 J. A. Christensen, B. T. Phelan, S. Chaudhuri, A. Acharya, V. S. Batista and M. R. Wasielewski, Phenothiazine Radical Cation Excited States as Super-oxidants for Energy-Demanding Reactions, *J. Am. Chem. Soc.*, 2018, **140**, 5290–5299.

5 C. Yang, D. Liu and R. R. Lunt, How to Accurately Report Transparent Luminescent Solar Concentrators, *Joule*, 2019, 3, 2871–2876.

6 M. G. Debije, R. C. Evans and G. Griffini, Laboratory protocols for measuring and reporting the performance of luminescent solar concentrators, *Energy Environ. Sci.*, 2021, 14, 293–301.

7 F. Corsini, A. Nitti, E. Tatsi, G. Mattioli, C. Botta, D. Pasini and G. Griffini, Large-Area Semi-Transparent Luminescent Solar Concentrators Based on Large Stokes Shift Aggregation-Induced Fluorinated Emitters Obtained Through a Sustainable Synthetic Approach, *Adv. Opt. Mater.*, 2021, **9**, 2100182.